Thesis Proposal

Kurtis Anstey
V00939802
Department of Physics and Astronomy
University of Victoria
November 17, 2020

Dr. Jody Klymak
Dr. Steven Mihaly
Dr. Richard Thomson

Contents

1 Introduction

This research will characterise the internal wave field at Barkley Canyon, off the coast of Vancouver Island, to provide information regarding regional mixing processes and what drives them. This is important for understanding transport of nutrients, heat, O_2, and CO_2, which affect both climate and biological productivity. This research makes use of time-series data of unique temporal and spatial characteristics, to build on a body of research regarding interactions of internal waves with canyon topography, and related processes, in the Vancouver Island Continental Shelf region.

1.1 Internal waves

Internal waves are slow-moving, low-frequency, underwater gravity waves that exist due to density gradients in the ocean interior (Garrett & Munk, 1979). They can have wavelengths up to kilometres long, and oscillate in a range between the Coriolis and Brunt–Väisälä (buoyancy) frequencies (Garrett & Munk, 1979). They are often caused by the wind, or tides and currents, moving over irregular seafloor topography, generating waves that travel outward through the stratified ocean (Hendershott & Garrett, 2018). These waves propagate through the depths, where incident topography can cause them to scatter, reflect, or break (Martini et al., 2013).

In physical oceanography internal waves are regular features. As early as the mid-19th century, scientists such as Stokes and Rayleigh were discussing fluid densities and stratification (Garrett & Munk, 1979). Internal waves were reported as consistent noise in early 20th-century hydrocast readings, and Ekman made note of them in his writings on fluid mechanics (Garrett & Munk, 1979). Later, Garrett and Munk (1979) developed the Garrett-Munk (GM) spectrum to define the characteristic frequency and wavenumber continuum of internal waves. As the capabilities of instruments has improved, scientists continue to uncover the importance of internal waves to both small- and large-scale physical processes (Garrett & Munk, 1979). As a result, there is much research opportunity; there are questions regarding internal wave generation and dissipation (Terker et al., 2014; Kunze, 2017), scattering and reflection on continental slopes (Nash et al., 2004; Kunze et al., 2012; Gemmrich & Klymak, 2015), and forcing response due to seasonal weather variability (Alford et al., 2012; Thomson & Krassovski, 2015), many of which involve internal waves interacting with topography.

As internal waves and tides approach coastal topography their energy is focused, and cascades from low- to high-frequency processes, eventually dissipating as heat (Garrett & Munk, 1979). This dissipation creates an energetic local environment, evident as turbulent processes on the micro- (less than 1 m vertical) and fine-scales (1 m to 100 m vertical) (Garrett & Munk, 1979; Kunze et al., 2012). This then contributes to the regional transport of energy and momentum, and the mixing of heat, pollutants, and biological constituents (Kunze et al., 2012). Furthermore, internal waves help to set ocean stratification, layers that drive large-scale systems such as overturning circulation (Garrett & Munk, 1979). As such, understanding internal wave interactions with topography is important to help predict changes in many facets of the coupled ocean-atmosphere climate system (Garrett & Munk, 1979).

Topography related internal wave studies have been ongoing at the Hawaiian ridge (Alford et al., 2007), in the South China Sea (Klymak et al., 2011), and in the canyons of the eastern Pacific (Allen et al., 2001; Carter & Gregg, 2002; Kunze et al., 2012; Terker et al., 2014). Canyons have been found to be hot spots of internal wave activity, that not only generate (Carter & Gregg, 2002), but also dissipate internal waves (Allen et al., 2001), focusing energy into high-frequency processes. Research in Monterey Canyon, California, has led to results regarding critical slopes scattering and reflecting incoming internal waves (Kunze et al., 2012), the presence of internal-bores and near-bottom turbulent layers that drive mixing (Carter & Gregg, 2002), and correlation between topography and increased dissipation and generation of internal waves and tides (Terker et al., 2014). This much information from a single site bodes well for further research at other canyons.

The success of topographic internal wave studies has led to research up the northeast Pacific coast (Martini et al., 2013; Allen et al., 2001); including Canada, where research is focused on the Vancouver Island Continental Shelf (VICS). Studies have led to information on seasonal wind forcing for near-inertial internal waves (Alford et al., 2012), potential evidence of non-linear wave-wave interaction between inertial and semidiurnal internal waves (Mihaly et al., 1998), and regional currents associated with the northeast Pacific current cycle (Thomson & Krassovski, 2015). The seasonally variable currents have been associated with observations of vorticity and upwelling in Barkley Canyon, suggesting considerable canyon influence on local water properties and regional transport of biological constituents (Allen et al., 2001). As such, further research at Barkley Canyon may improve understanding of regional processes associated with internal waves, and what drives them.

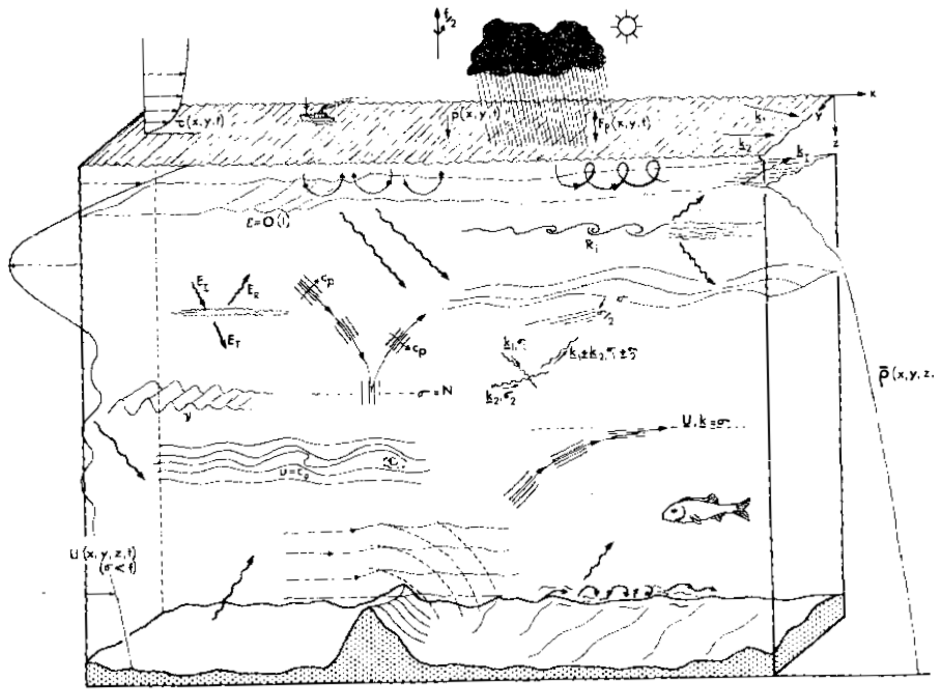

Figure 1: General depiction of internal wave processes in the ocean, as envisioned by Garrett and Munk (1979).

1.2 Barkley Canyon

The data for this research is from Barkley Canyon, and is unique for both temporal and spatial consideration. Located at approximately 48.33°N 126.03°W, Barkley Canyon is about 100 km southwest of Vancouver Island, with a rim and axis at depths of approximately -400 and -900 m, respectively (Barkley Canyon, 2013). Spread throughout the topography of the canyon, Acoustic Doppler Current Profilers (ADCP) provide velocity data for Ocean Networks Canada (ONC), which maintains the array of ADCP and other instruments (ONC, 2013). The available time series is over ten years, much longer than is typically available for internal wave research, allowing for analysis of multi-year and decadal variability. Furthermore, the placement of multiple ADCP allows for spatial analysis of internal wave effects through the canyon, typically difficult with only a single instrument or dropped observations.

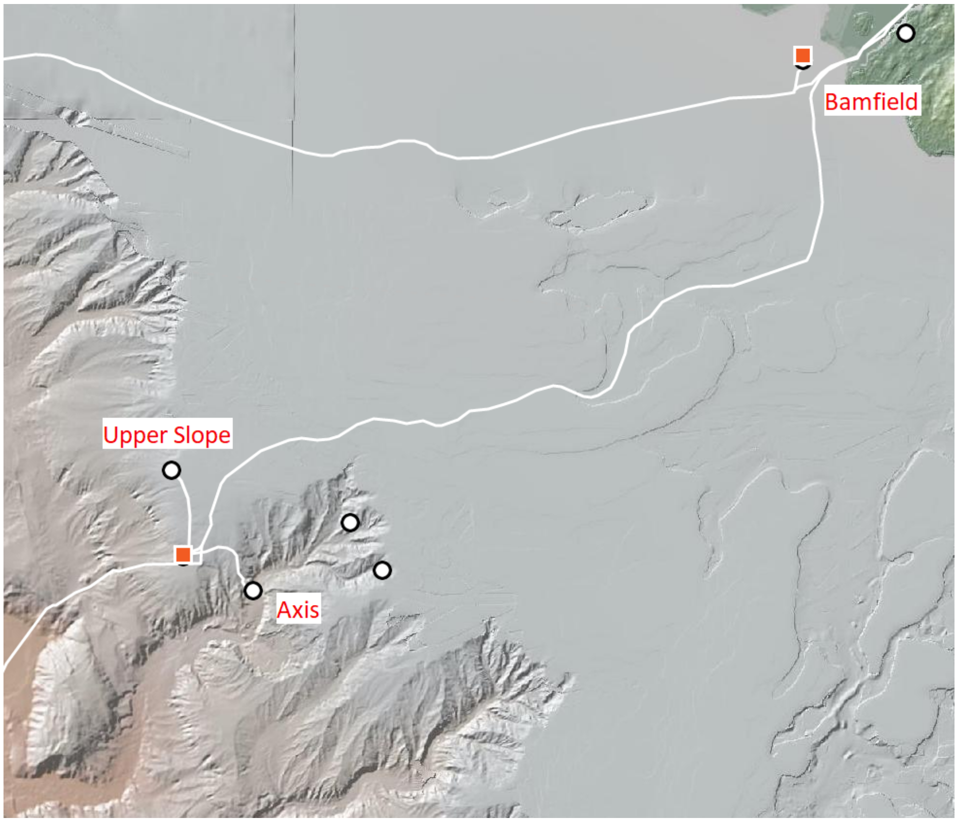

Figure 2: General map of the Barkley Canyon region, about 100 km southwest of Bamfield, Vancouver Island. Circles represent local ONC instrument moorings, with the relevant Axis and Upper Slope ADCP instruments indicated. Adapted from the ONC Oceans 2.0 data portal (ONC, 2020).

1.3 Data acquisition

Acoustic Doppler Current Profilers (ADCP) emit acoustic beams that triangulate Doppler shifts in the water column, providing directional velocity data over time. For Barkley Canyon, the ONC Oceans 2.0 data portal offers publicly available data spanning over 10 years, from 2009 to present, at a sampling rate of 2-seconds. The ADCP and their data are configured and cleaned by ONC. Relevant ADCP were chosen as the Axis (75 kHz and 55 kHz), Upper Slope (75 kHz), and Mid-East (150 kHz) nodes. Complete datasets were downloaded in NetCDF format at a resolution of 1-hour, to check data quality. Some issues were noted with the Mid-East 150 kHz beams, and sent to ONC for revision, and are pending review. Otherwise, Axis 75 kHz and Upper Slope 75 kHz both offer reliable data, and these two instruments will be the primary sources for this research. There are a few instances of data gaps, and NaN values near the extrema of beam range, which will be accounted for during analysis. Overlapping good quality coverage is primarily during 2013, 2014, 2017, and 2018, and certain comparisons will be possible for other years and seasons. Furthermore, the potential use of the Axis 55 kHz (pending conversion) and Mid-East 150 kHz (pending ONC revision) could add to this coverage, if necessary.

Axis - 75 kHz ADCP - Depth 968 metres (near canyon bottom)
Upper Slope - 75 kHz ADCP - Depth 378 metres (canyon adjacent plateau)

After the initial quality check, complete datasets for Axis 75 kHz and Upper Slope 75 kHz ADCP were downloaded in NetCDF format at a resolution of 15-minutes, determined to be adequate averaging of the data required for the science objectives of this research.

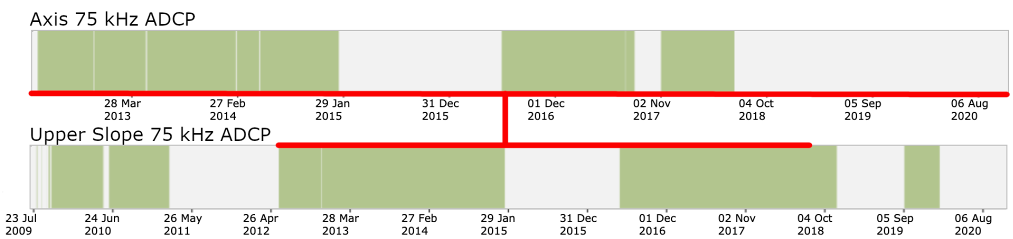

Figure 3: Data coverage for the Axis 75 kHz and Upper Slope 75 kHz ADCP. Primary overlap of good quality data is in 2013, 2014, 2017, and 2018. Adapted from the ONC Oceans 2.0 data portal (ONC, 2020).

2 Project goals

2.1 Thesis

This research seeks to characterise the internal wave field at Barkley Canyon, near Vancouver Island, to provide information regarding local and regional mixing processes, and, ideally, what drives them. This will include an analysis of variability in regional mean currents, tides, and winds, to identify forcing. Forcing will be correlated to observable internal wave events within the canyon, and association expanded to dissipative processes that may affect regional systems.

- We will evaluate velocity data for temporal and spatial trends, to identify forcing. We will examine low-pass filtered velocity data to identify regional mean currents, such as the VICS segment of the Northeast Pacific Coastal Current (NPCC), and notable events will be compared with weather data. We will conduct a similar analysis of super-inertial velocity data to identify prominent tidal constituents. We will also evaluate the direction and depth of these flows for topographic dependencies.

- We will use spectral analysis (power spectra, rotary spectra, and spectrograms), in both 1D and 2D, to provide estimates of the relative power, rotation, and seasonal dependencies of notable frequency constituents. Temporally, we will compare spectra to seasonal forcing by the wind, mean currents, and tides, at time scales ranging from seasonal to decadal. We will also compare spectra at various depths to investigate topographic dependencies.

- We will characterise the continuum to compare with observed seasonality, to check for its presence in the broadband. As the state of the continuum is thought to be related to the rate of energy dissipation in the system, we will attempt to correlate seasonal variability in energy levels to local dissipation rates (Carter & Gregg, 2002). We will also compare the characterised continuum with the classical open ocean GM spectrum, calibrated for local climatology.

2.2 Optional goals

There are many other forms of internal wave analysis that could be included to expand on the proposed goals, but that may be beyond the limited scope of this research as an MSc project. Optional goals could include:

- An analysis of critical slope angles for the VICS near the Barkley Canyon mouth, and the efficiency of associated internal wave reflection and/or scattering in this region.

- A search for evidence of non-linearity in the time series, which could suggest non-linear wave-wave interaction between wind generated downward internal waves and canyon generated upward internal tides (Mihaly et al., 1998).
- A report to ONC with useful data quality assessment, instrument calibration feedback, and data analysis processes, to assist in the successful outcomes of continued research along the VICS.

2.3 Prospective timeline

- December 2020: Complete final required course.
- January 2021: Complete preliminary analysis. Begin writing thesis.
- March/April 2021: Finish thesis. Schedule thesis defence.
- May/June 2021: Defend thesis.

3 Preliminary methods and analysis

All plots and analyses are works-in-progress, and are only samples to highlight the potential of this research.

Preliminary analysis has been carried out using ONC Oceans 2.0 for data acquisition, Python and Jupyter Notebook for data processing, LaTeX and BibDesk for document creation, and GitHub (kurtisanstey/project) for file hosting. Other relevant packages and resources are mentioned when necessary.

Details can be found in the relevant Jupyter Notebook project files, and a comprehensive list of preliminary results can be found in the Analysis document, both hosted on GitHub. Each form of analysis is available for time scales ranging from seasonal to decadal, per and between instruments.

3.1 Velocities

Velocity data were truncated and NaN values interpolated to improve temporal quality, and to remove noise at the extreme depth limits of each instrument. Data were filtered to highlight differences in the mean currents and tides, by applying a 40-hour digital low-pass Butterworth filter and examining the low-pass versus the super-inertial data. Data were rotated using Euler's formula

$$\underline{u}_{rot} = \underline{u}e^{-i\theta}$$

to better match the cross-slope angle of approximately +30°, to help identify relationships between the predominant VICS currents and local canyon topography; u is referred to as 'cross-slope', and v is 'along-slope'.

Potential trends in Upper Slope (-330 m to -100 m) velocity data include a seasonal switch in mean currents from NW to SE during the spring, potentially corresponding to variability in the NPCC. There are apparent two-week pulses that could correspond with the spring-neap cycle. For Axis (-900 m to -400 m) there is less seasonality, and fairly consistent flow into the canyon near the floor and back out closer to the rim. Comparatively, velocities are dominant in the along-slope direction for Upper Slope, and cross-slope for Axis.

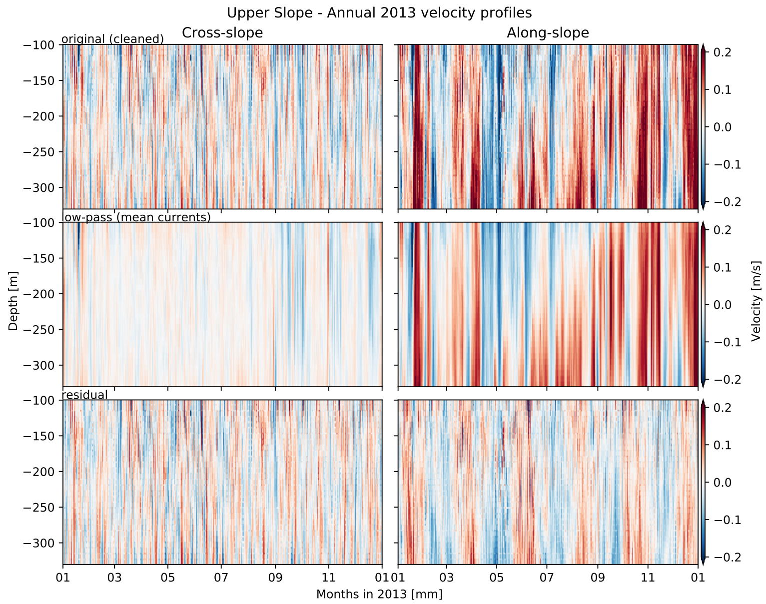

(a) Upper Slope - 2013

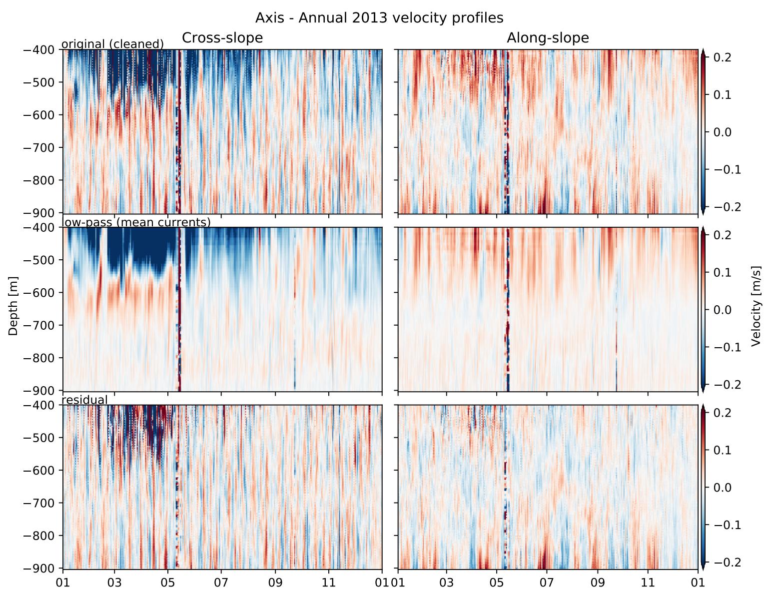

(b) Axis - 2013

Figure 4: Sample velocity data for Upper Slope 75 kHz and Axis 75 kHz ADCP, in 2013. Velocities are displayed horizontally in cross- (left) and along-slope (right) directions, and vertically as unfiltered (top), 40-hour low-pass (middle), and residual (bottom) data. The 15-minute resolution velocity data was cleaned to account for NaN gaps and extreme depth interference, and rotated to match the continental slope angle of approximately 30°.

3.2 Spectral analysis

Power spectral density (PSD) plots were created from rotated, cleaned, and mean removed velocity data. A Welch method FFT process was used, with averaging parameters set according to the length of each data set, and a 15-minute sampling rate for ideal smoothing of spectral features. For reference, also plotted are notable frequency constituents, 95% confidence intervals, expected continuum slopes, and depth-average spectra. Specific depths were selected as the upper and lower extrema of depth values obtained by each ADCP, after being truncated to remove noise.

Rotary spectra were created from similar data as for PSD, and based on the work of Thomson (2014) and Gonella (1972) to determine CW and CCW components, and better inspect inertial contributions. Additional rotary analysis plots will be developed in 2D for time and depth, after 1D analysis has been properly calibrated.

Spectrograms were generated using similar methods and parameters as for PSD, and 'whitened' for visual clarity (multiplying spectrogram output by frequency squared).

The classical GM spectrum for this region was generated from buoyancy data from seasonal CTD casts by Fisheries and Oceans Canada (DFO), at Line P Station P4, about 27 km from Barkley Canyon. The characteristic spectrum is still being calibrated for local water properties, for comparison.

Potential PSD trends include a depth dependence for tidal constituents - and some seasonal dependence - with M_2 dominating overall, and f weakening at lower depths. There is a 'flattening' of the continuum at higher frequencies that could be associated with the instrument noise floor (to be determined). For Upper Slope, there are sum peaks for fM_2 and M_4. For Axis, there are three consistent high frequency peaks that have yet to be evaluated.

Potential Upper Slope spectrogram trends include a lack of high-frequency activity in the summer, possibly corresponding to a lack of storms. Though seasonality is less evident in the cross-slope direction, this direction also features more consistent high-frequency activity. Axis appears to show less seasonality, as evident in PSD findings, which likely corresponds to a depth dependence on wind effects.

Preliminary rotary spectra for Upper Slope show CW components dominating, with the inertial constituent absent in the CCW direction, as expected. Spectral features are similar to the PSD, with evident sum peaks and depth dependence for tidal constituents.

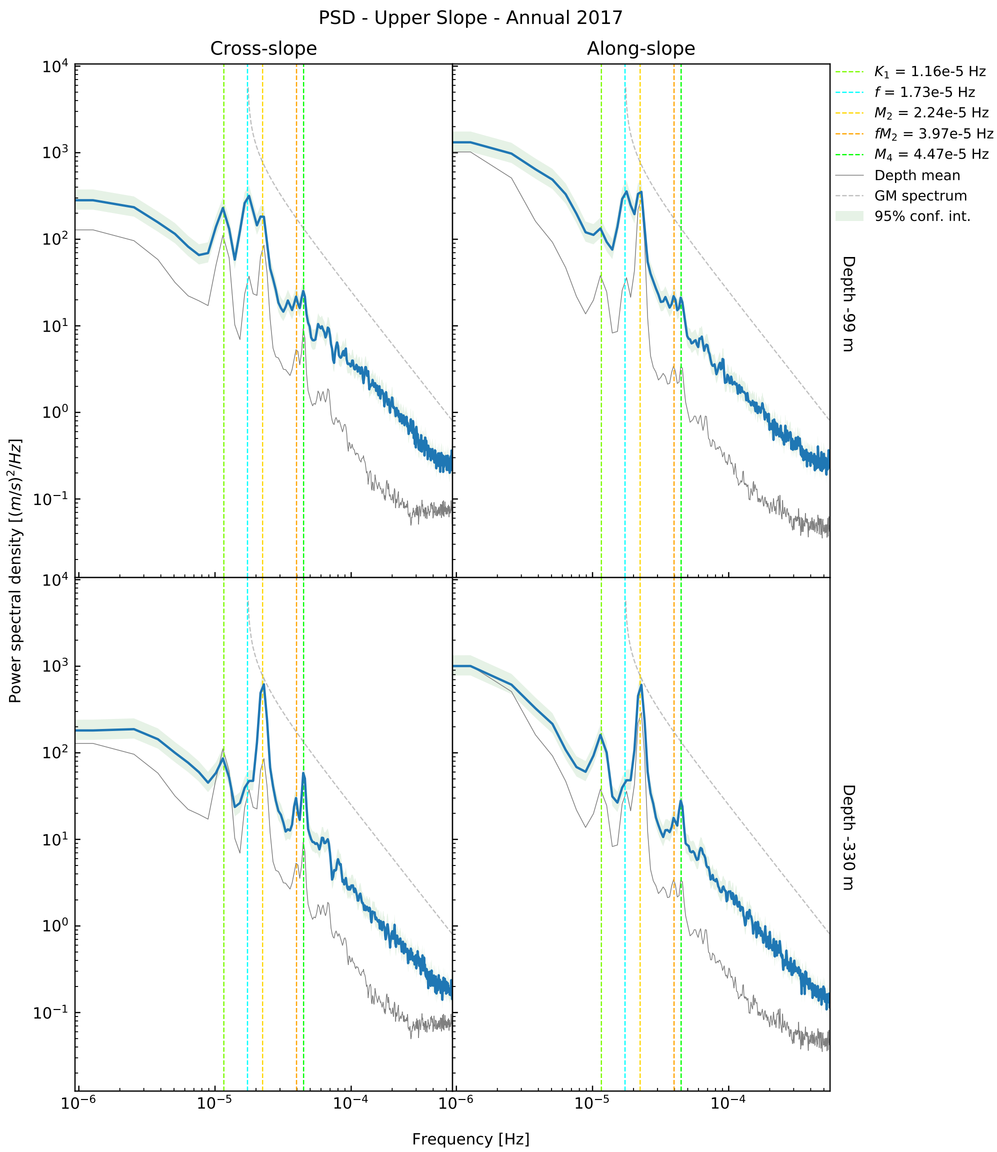

Figure 5: Sample PSD data for Upper Slope 75 kHz ADCP, in 2017. PSD show the cross- (left) and along-slope (right) velocity data, at an upper depth of -99 m (top) and lower depth of -330 m (bottom). PSD were processed using mean-removed, rotated, and cleaned velocity data, and optimised Welch FFT parameters. The GM spectrum is for reference only, and is still being calibrated for local water properties.

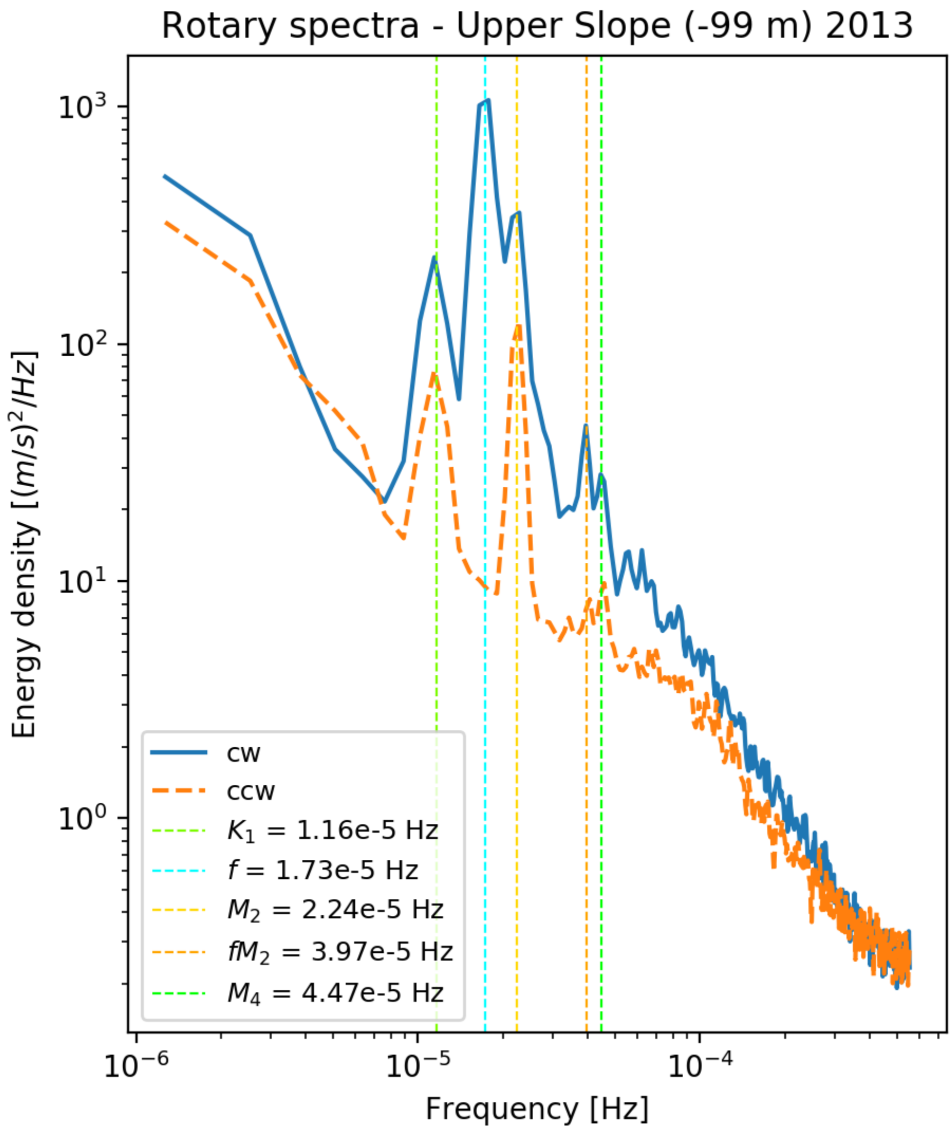

Figure 6: Sample rotary spectra for Upper Slope 75 kHz ADCP, at -99 m depth, in 2013. Spectra were processed using mean-removed, rotated, and cleaned velocity data, and averaged PSD and CSD parameters in a personally developed process based on Thomson (2014) and Gonella (1972). Rotary spectra are for reference only, and are still being calibrated for appropriate comparison.

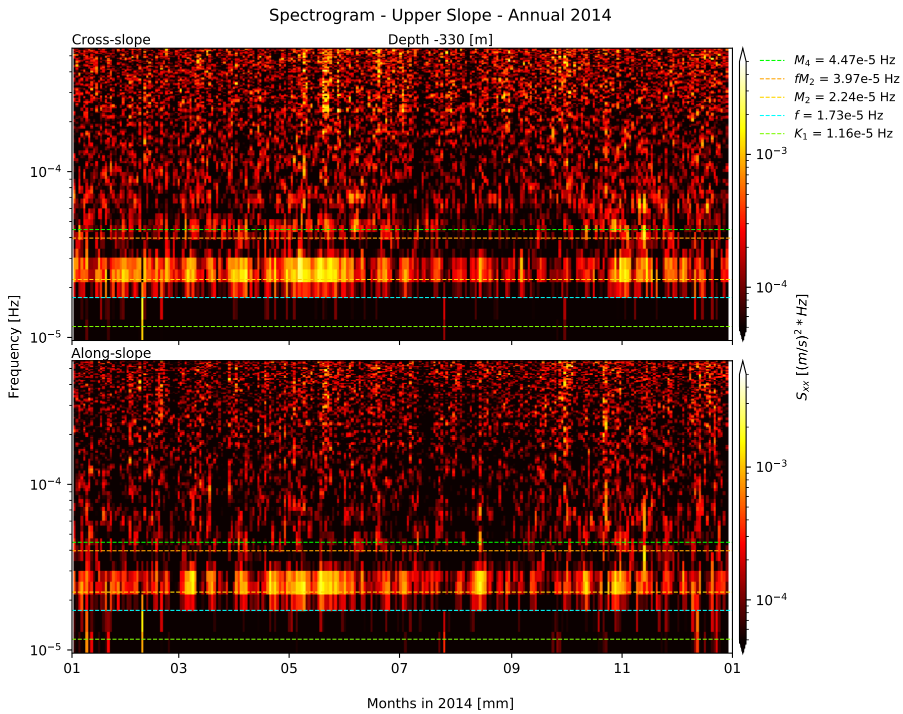

Figure 7: Sample spectrogram data for Upper Slope 75 kHz ADCP, at -330 metres depth, in 2014. Spectrograms are for the cross- (upper) and along-slope (lower) velocity data. Spectrograms were processed using mean-removed and cleaned velocity data (see above), optimised Welch FFT parameters, and 'whitened' for visual clarity.

3.3 Buoyancy and density

Climatology data from annual Line P cruises allow for buoyancy and density calculations through depth, which can provide insight into the structure of the water column. CTD data were obtained from La Perouse/Line P cruises. Barkley Canyon is centred at approximately 48.33°N 126.03°W, so Rosette (deep) CTD casts from Station P4 are closest (approximately 48.39°N 126.39°W); a distance of about 27 km. Winter CTD casts were within January/February, and summer casts were within August/September. The Seawater package was used to calculate density, $\rho(z)$, and the Brünt-Väisälä Frequency squared ($N^2(z)$), based on the UNESCO 1983 (EOS 80) polynomial, at the mid-depths from the equation:

$$N^2 = \frac{-g}{\sigma_\theta}\frac{d\sigma_\theta}{dz}$$

where σ_θ is the density based on potential temperature values.

These N^2 values were then applied to a modified Python GM toolbox to generate a GM spectrum based on local climatology, that is currently being adapted for comparison with spectra.

There is some general seasonality in the buoyancy data, with far more variability in upper depths above -200 metres, particularly in the summer. However, variability in depths above -200 m is mostly irrelevant for ADCP data that is primarily between -900 m and -100 m. Buoyancy frequency (N^2) values are fairly static below -200 m at approximately 1×10^{-5} $(rad/s)^2$.

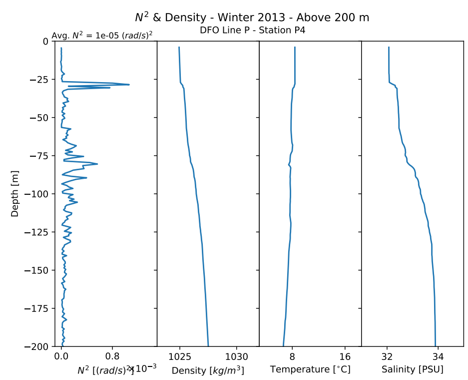

(a) Upper Winter

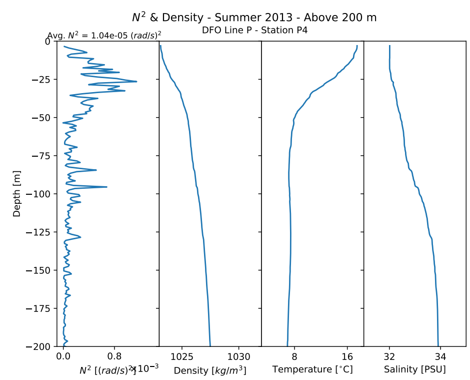

(b) Upper Summer

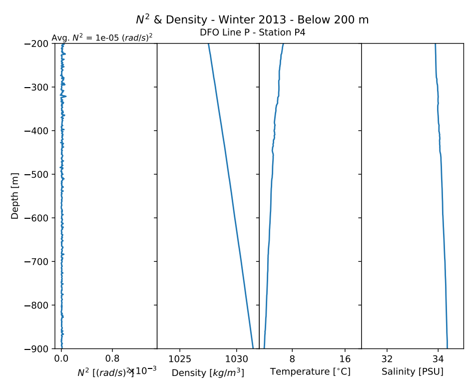

(c) Lower Winter

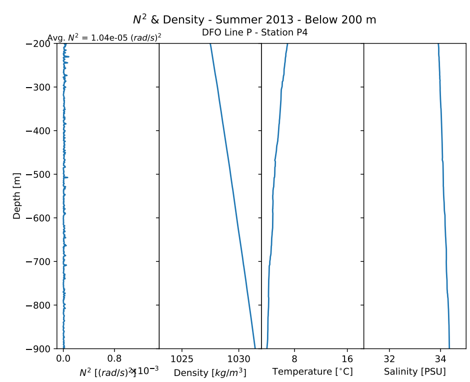

(d) Lower Summer

Figure 8: Sample plots of seasonal N^2 and CTD data for Station P4 of Line P, collected by DFO in 2013. The top row is for depths above -200 m, and the bottom row below -200 m. Each plot shows N^2, density, temperature, and salinity, in order.

4 Relevant reading

Alford, M. H., Mackinnon, J. A., Zhao, Z., Pinkel, R., Klymak, J., Peacock, T., . . . Peacock, T. (2007). Internal waves across the Pacific. Geophys. Res. Lett, 34, 24601. https://doi.org/10.1029/2007GL031566

Alford, M. H., Cronin, M. F., & Klymak, J. M. (2012). Annual cycle and depth penetration of wind-generated near-inertial internal waves at ocean station papa in the northeast pacific. Journal of Physical Oceanography, 42(6), 889–909. https://doi.org/10.1175/JPO-D-11-092.1

Allen, S. E., Vindeirinho, C., Thomson, R. E., Foreman, M. G. G., & Mackas, D. L. (2001). Physical and biological processes over a submarine canyon during an upwelling event. Canadian Journal of Fisheries and Aquatic Sciences, 58(4), 671–684. https://doi.org/10.1139/f01-008

Carter, G. S., & Gregg, M. C. (2002). Intense, Variable Mixing near the Head of Monterey Submarine Canyon. In Journal of Physical Oceanography (Vol. 32). https://doi.org/10.1175/1520-0485(2002)032¡3145:IVMNTH¿2.0.CO;2

Garrett, C., & Munk, W. (1979). Internal Waves in the Ocean. Ann. Rev. Fluid Mech., 11, 339–369.

Gemmrich, J., & Klymak, J. M. (2015). Dissipation of internal wave energy generated on a critical slope. Journal of Physical Oceanography, 45(9), 2221–2238. https://doi.org/10.1175/JPO-D-14-0236.1

Gilmour, A. (1987). A preliminary rotary spectral analysis of inertial currents off the west coast of New Zealand. New Zealand Journal of Marine and Freshwater Research, 21, 353–357. 10.1080/00288330.1987.9516231

Gonella, J. (1972). A rotary-component method for analysing meteorological and oceanographic vector time series (Vol. 19). Pergamon Press.

Hendershott, M., & Garrett, C. (2018). Lecture 6: Internal tides. Geophysical Fluid Dynamics, Woods Hole Oceanographic Institute. Retrieved from https://gfd.whoi.edu/wp-content/uploads/sites/18/2018/03/lecture0621356.pdf

Kelly, S., Nash, J., & E.Kunze. (2010). Internal-tide energy over topography. J. Geophys. Res., 115, C06014. doi.org/doi:10.1029/2009JC005618

Klymak, J. M., Alford, M. H., Pinkel, R., Lien, R. C., Yang, Y. J., & Tang, T. Y. (2011). The breaking and scattering of the internal tide on a continental slope. Journal of Physical Oceanography, 41(5), 926–945. https://doi.org/10.1175/2010JPO4500.1

Kunze, E. (2017). Internal-wave-driven mixing: Global geography and budgets. Journal of Physical Oceanography, 47(6), 1325–1345. Retrieved from https://doi.org/10.1175/JPO-D-16-0141.1

Kunze, E., Mackay, C., Mcphee-Shaw, E. E., Morrice, K., Girton, J. B., & Terker, S. R. (2012). Turbulent mixing and exchange with interior waters on sloping boundaries. Journal of Physical Oceanography, 42(6), 910–927. https://doi.org/10.1175/JPO-D-11-075.1

MacKinnon, J., Zhao, Z., Whalen, C., Waterhouse, A., Trossman, D., Sun, O., . . . Alford, M. (2017). Climate process team on internal wave-driven ocean mixing. Bulletin of the American Meteorological Society, 98(11), 2429–2454. doi.org/10.1175/BAMS-D-16-0030.1

Martini, K. I., Alford, M. H., Kunze, E., Kelly, S. M., & Nash, J. D. (2013). Internal bores and breaking internal tides on the Oregon continental slope. In Journal of Physical Oceanography (Vol. 43). https://doi.org/10.1175/JPO-D-12-030.1

Mihaly, S., Thomson, R., & Rabinovich, A. (1998). Evidence for nonlinear interaction between internal waves of inertial and semidiurnal frequency. Geophysical Research Letters, 25(8), 1205–1208. Retrieved from https://doi.org/10.1029/98GL00722

Munk, W., & Garret, C. (1979). 9: Internal Waves and Small-Scale Processes.

Nash, J., Kunze, E., Toole, J., & Schmitt, R. (2004). Internal Tide Reflection and Turbulent Mixing on the Continental Slope. American Meteorological Society. Retrieved from http://journals.ametsoc.org/jpo/article-pdf/34/5/1117/4470231/1520-0485

Ocean Networks Canada. (2013). Barkley Canyon. Retrieved from https://www.oceannetworks.ca/introduction-barkley-canyon

Ocean Networks Canada. (2020). Oceans 2.0. Retrieved from https://data.oceannetworks.ca/DataSearch

Rainville, L., & Pinkel, R. (2006). Propagation of Low-Mode Internal Waves through the Ocean. Retrieved from http://journals.ametsoc.org/jpo/article-pdf/36/6/1220/4483319/jpo28891.pdf

Robertson, R., Dong, J., & Hartlipp, P. (2017). Diurnal Critical Latitude and the Latitude Dependence of Internal Tides, Internal Waves, and Mixing

Based on Barcoo Seamount. Journal of Geophysical Research: Oceans, 122(10), 7838–7866. https://doi.org/10.1002/2016JC012591

Terker, S. R., Girton, J. B., Kunze, E., Klymak, J. M., & Pinkel, R. (2014). Observations of the internal tide on the California continental margin near Monterey Bay. Continental Shelf Research, 82, 60–71. https://doi.org/10.1016/j.csr.2014.01.017

Thomson, R. E., & Emery, W. J. (2014). Data analysis methods in physical oceanography (Third ed.). Oxford, UK; Elsevier.

Thomson, R. E., & Krassovski, M. V. (2015). Remote alongshore winds drive variability of the California Undercurrent off the British Columbia-Washington coast. Journal of Geophysical Research: Oceans, 120(12), 8151–8176. https://doi.org/10.1002/2015JC011306